

Pictorial essay:

All rights reserved © K H Fung / Tridactyls.org

VIRTUAL AUTOPSY OF NAZCA TRIDACTYL MUMMY ‘SEBASTIAN’

A scientific study using CT scan with advanced 3D image reconstruction and virtual dissection.

By **Dr. K.H. Fung** (Hong Kong SAR, China)

December 2025

ACKNOWLEDGEMENT

- The author wished to thank Tridactyls.org for granting permission for use of the DICOM CT datasets available on their website for this scientific study.

SECTION I: STATE OF THE MUMMY ‘SEBASTIAN’

- ‘Sebastian’ is a very well preserved, desiccated and complete corpse found in the Peruvian desert in Nazca in 2023 (strictly speaking not a mummy as commonly mentioned).
- The gender cannot be definitively verified based on CT.
- It was found in a foetal position. (*Figure 1 &2*) The contracted and detached bi-lobed brain remnant was located in posterior aspect of the cranium suggesting that it had been in a dependent supine posture with head tilted towards the right side after death. (*Figure 3*)
- Despite having grossly bipedal human characteristics ‘Sebastian’ had many anomalous features unlike normal modern human including cranio-facial abnormalities and tridactyl hands and feet. (*see below*)
- The closely integrated internal anatomy can be well identified on serial 2D CT scans as well as 3D reconstruction from the datasets pointing to genuine natural morphology.
- There were evidences of biological consequences to injury suggesting that it had once been a living biological entity.
- It had unfused epiphyses in long bones (*Figure 4*) and some unerupted teeth (*Figure 5*) consistent with an immature skeleton of a child. An ectopic tooth was found on anterior surface of left maxillary antrum. (*Figure 6*)
- A layer of outside material (some hyperdense on CT) was noted over perineal area.



Figure 1: 3D CT of 'Sebastian' showing its surface anatomy in various projections. Note the foetal posture, tridactyl hands and feet and presence of 3 metallic implants (*in orange colour*).



Figure 2: 3D CT of 'Sebastian' in semi-transparency showing skin, bones and metallic implants.

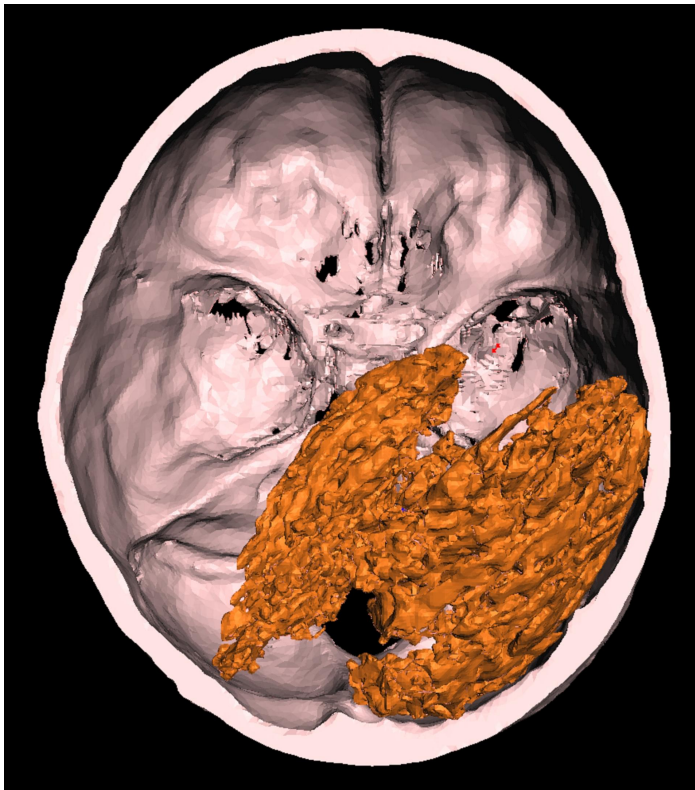


Figure 3: 3D CT of section of skull base. The bi-lobed brain remnant (*in orange colour*) can be seen in right side of posterior cranial cavity.



Figure 4: 3D CT of right lower limb showing presence of unfused epiphyses (*in lilac colour*) in long bones (*in yellow colour*). The skin is shown *in blue colour*. The tridactyl foot showed a more robust medial digit and weaker lateral digit. Note the wide spacing between the digits that is not found in human configuration. The counterparts of human metatarsal bones are incorporated into the digits. The tarsal bones arrangement remained similar to human configuration. Ligament and plantar fascia can still be found (*not shown*).

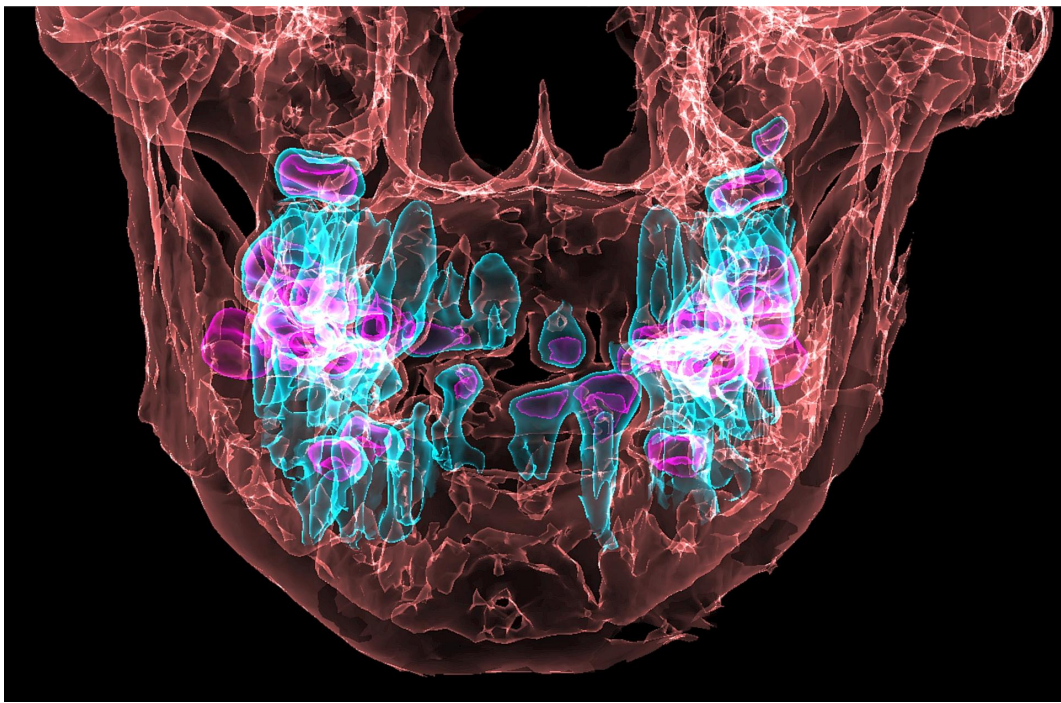


Figure 5: 3D CT scan of maxilla and mandible showing teeth (*in blue colour*), some remains unerupted. The crown of teeth are *in lilac colour*.

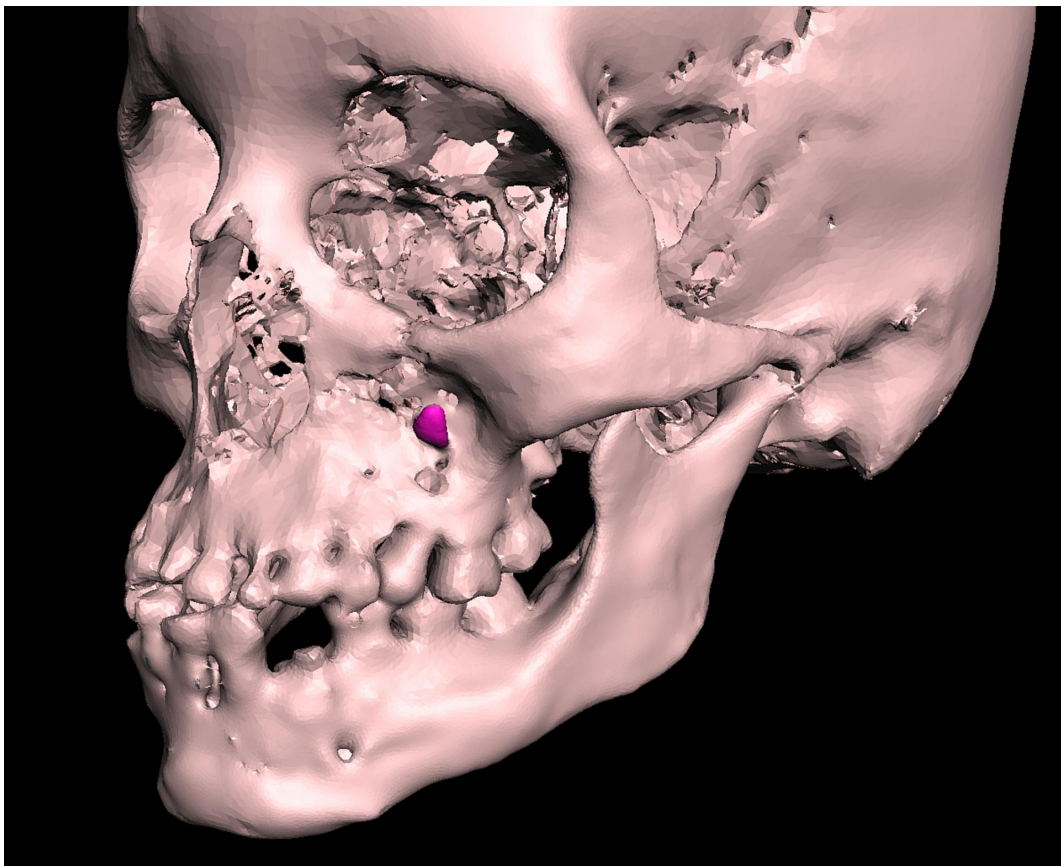


Figure 6: 3D CT scan of maxilla and mandible showing presence of an ectopic tooth (*in lilac colour*) overlying the anterior surface of the left maxillary bone. This is an extremely rare location to find ectopic tooth.

SECTION II: ANATOMICAL ANOMALIES IN ‘SEBASTIAN’

- ‘Sebastian’ showed abnormal facial appearance with widely separated large slanting eyelids, inconspicuous nose, bilateral flat nostrils pointing inferio-medially, relatively small face, protruding jaws and pointed chin, absence of external ear (pinnae), absence of external open in ear canals. *(Figure 7 & 8)*
- Fused cranial sutures. *(Figure 9)*
- Scattered tiny nodularities in scalp and skull bone. *(Figure 8 & 9)*
- Oval shaped but posteriorly enlarged foramen magnum. *(Figure 10)*
- Disk like metallic implant over bilateral clavicles with indentations. *(Figure 11)*
- Collar-like metallic implant in posterior neck showing relief markings on its outer surface. *(Figure 12)* There was suggestion of composite material with denser eccentric core. *(Figure 13)* Evidence of induced bone growth from spinous processes of C2 and to a minor extent C3 incorporating into the implant was evident. *(Figure 14)*
- Heavily calcified robust costal cartilages forming U-shaped deformity with depressed sternum (i.e. pectus excavatum). *(Figure 15)*
- Heavily calcified intervertebral disks in thoracic and lumbar spine. *(Figure 16, 38)*
- Prominent median fold in anterior abdominal wall. *(Figure 17)* Absence of navel.
- Wide flat triangular shaped perineum with lack of buttock prominences. *(Figure 18)*
- ‘Rocker bottom foot’ noted in left foot. *(Figure 19)*
- Seeds in coprolite. *(Figure 20)*
- Tiny focal calcification in left lung. *(Figure 21)*
- Bony defect suggestive of Tarlov cyst in left sacral foramina *(Figure 22)*

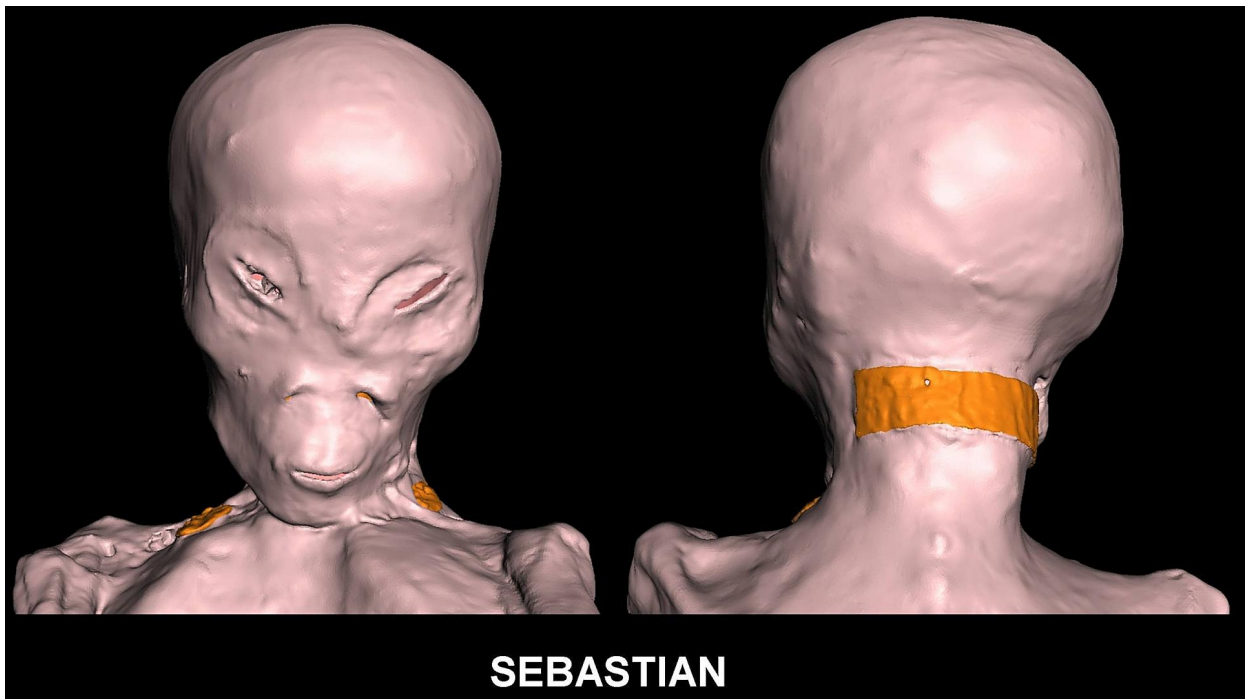


Figure 7: 3D CT showing front and back view of head. Note the widely separated large slanting eyelids, inconspicuous nose, flat downward and medial pointing nostrils, small face, prominent jaws and small pointed chin. Tiny skin nodules were noted in scalp and right side of face. Metallic implants were shown in orange colour.

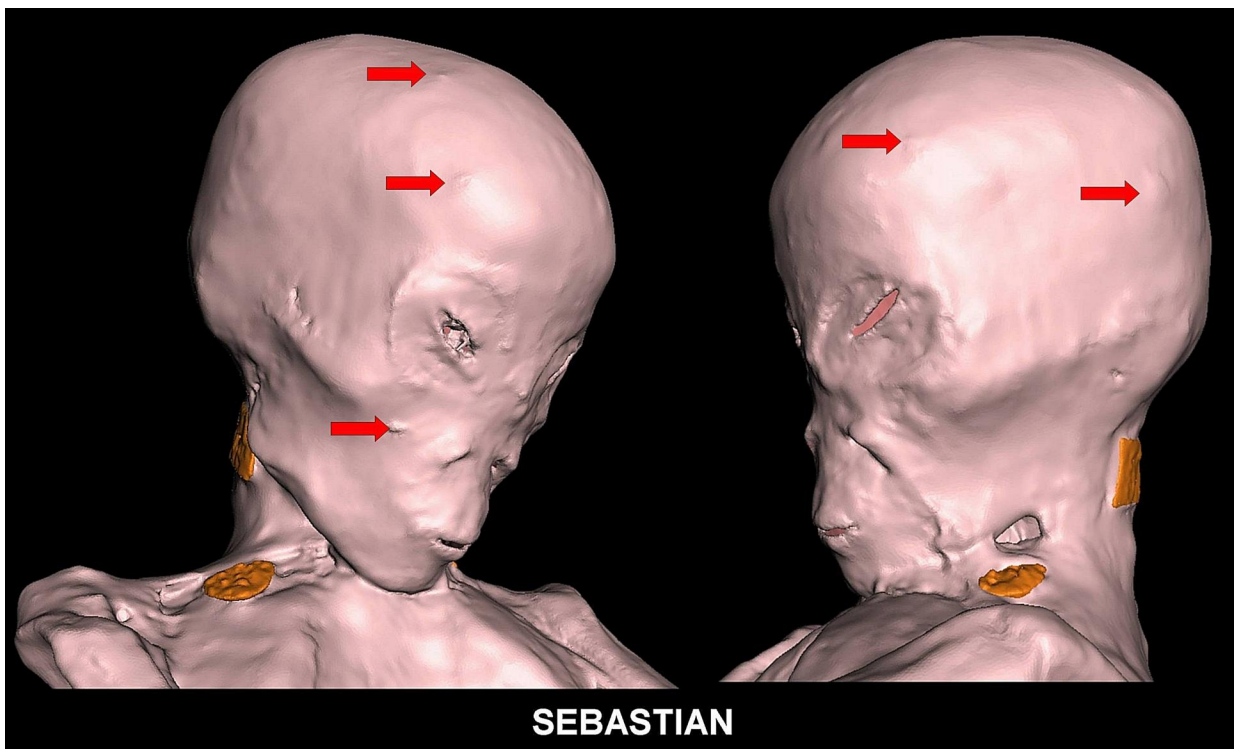


Figure 8: 3D CT showing oblique views of head and neck. Note absence of ear canal and pinnae. Metallic implants were shown in orange colour. Tiny skin nodules were noted in scalp bilaterally and in right face (*red arrows*).

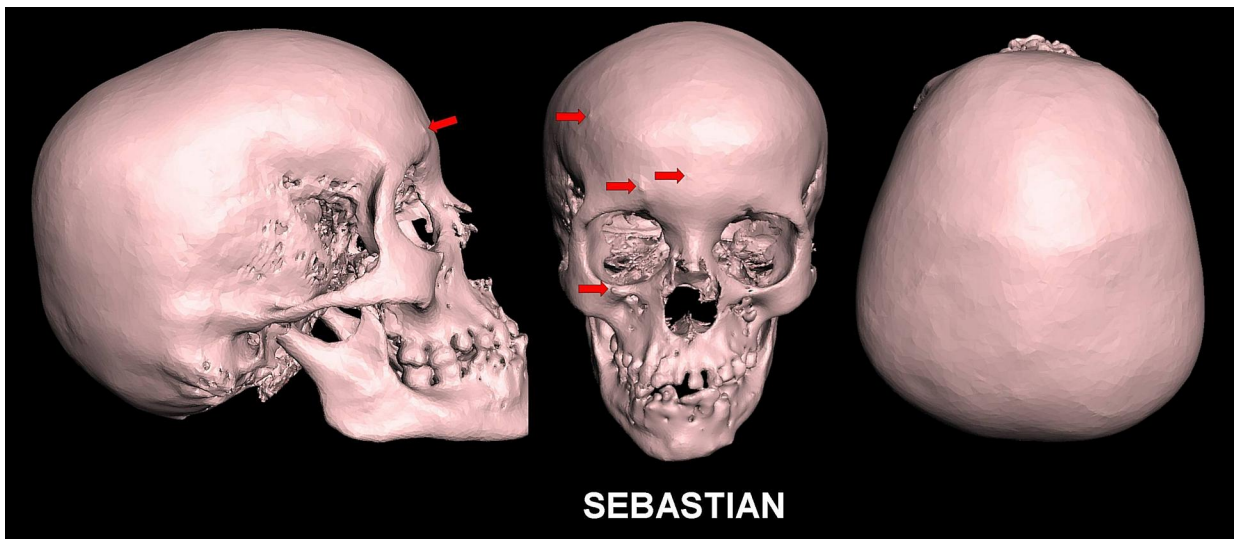


Figure 9: 3D CT showing right lateral (*left*), frontal (*middle*) and top views of skull (*right*). Cranial sutures were fused. No distinct skull sutures were visible on its surface. The cranium was not elongated. Facial bone were small with concave anterior surfaces. Orbits were enlarged. Prominent upper jaw showed asymmetry. Tiny bone nodules were noted in forehead and right facial bone (*red arrows*).

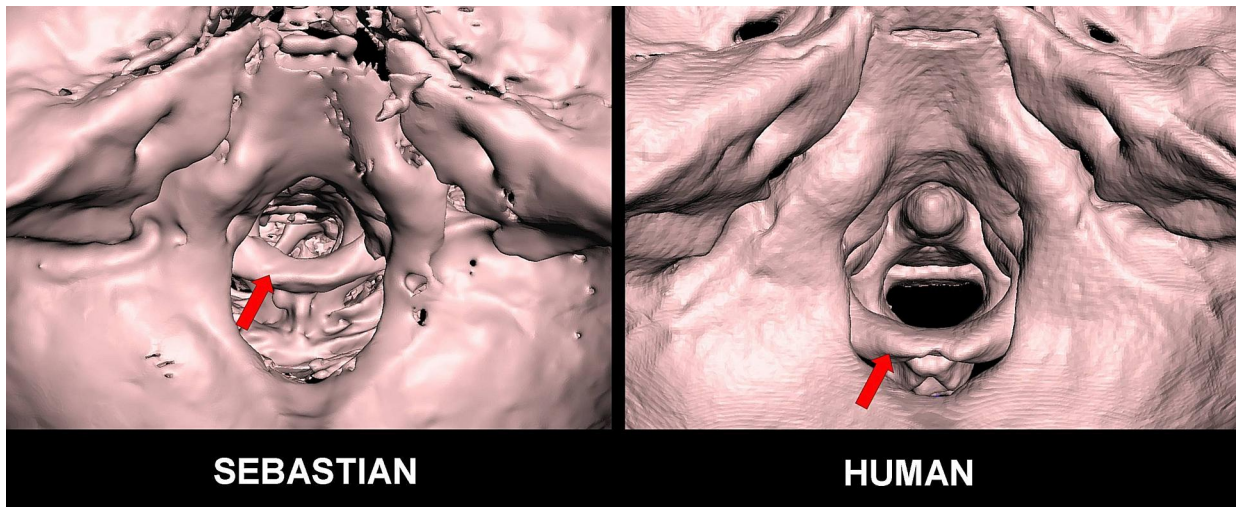


Figure 10: 3D CT showing foramen magnum viewed from above of ‘Sebastian’ comparing with modern human. Note the posterior extension of the foramen magnum in ‘Sebastian’ relative to the posterior arch of atlas (*red arrows*).

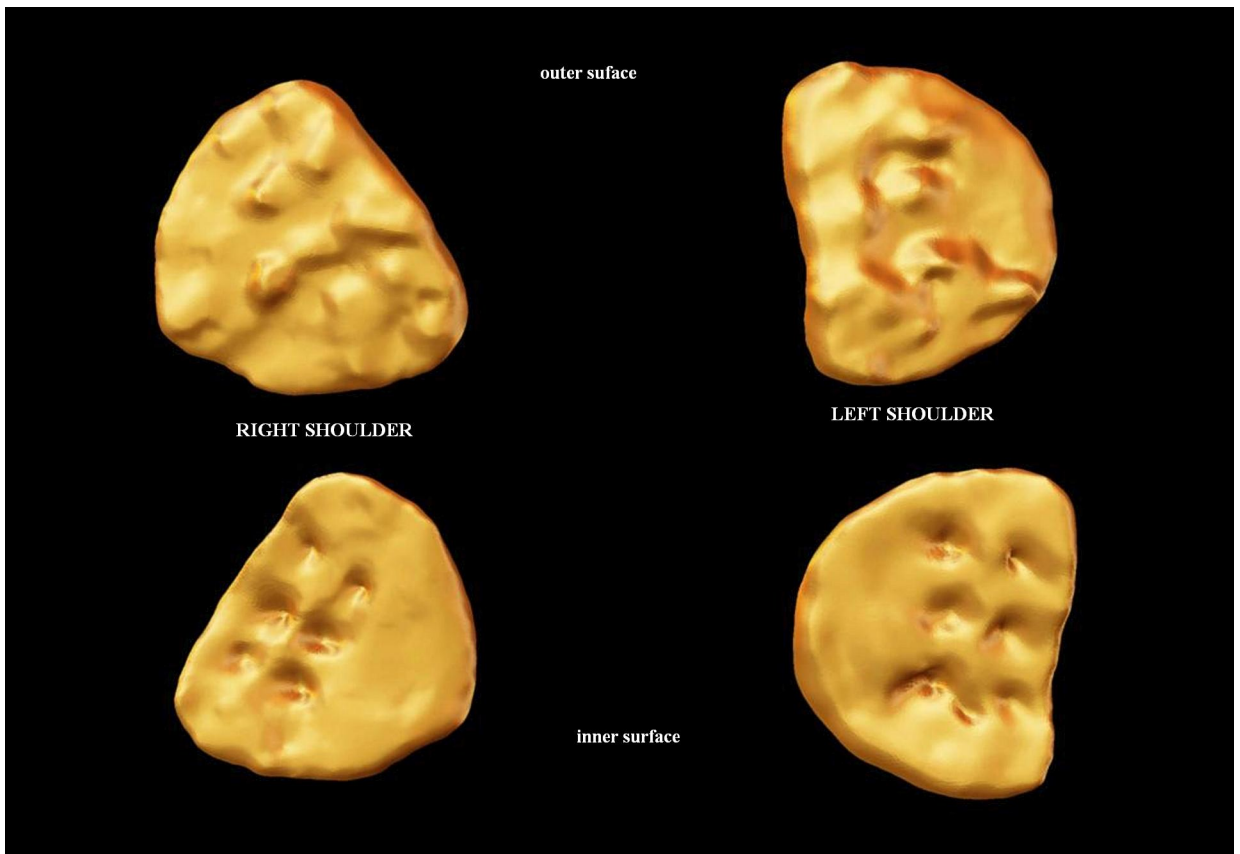


Figure 11: 3D CT showing disk shaped metallic implants with indentations overlying bilateral clavicles.

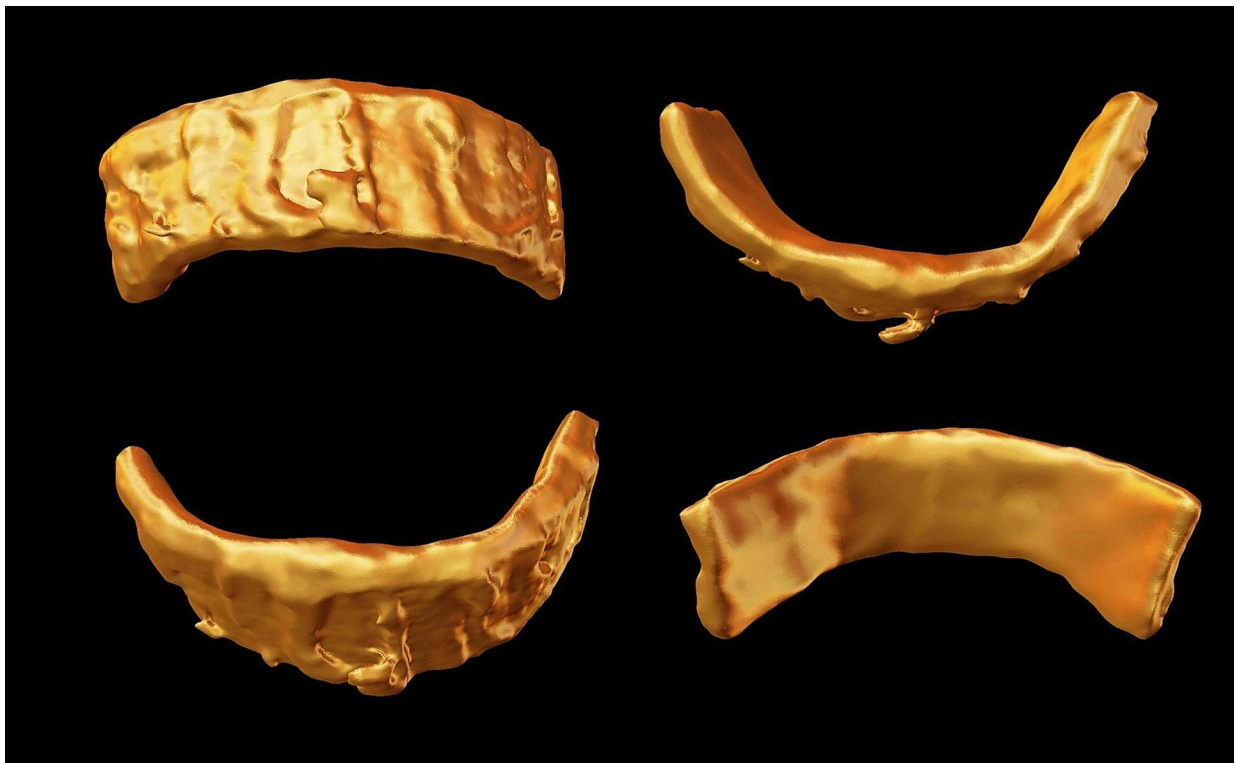


Figure 12: 3D CT showing collar-like metallic implant behind neck with relief markings on its outer surface.

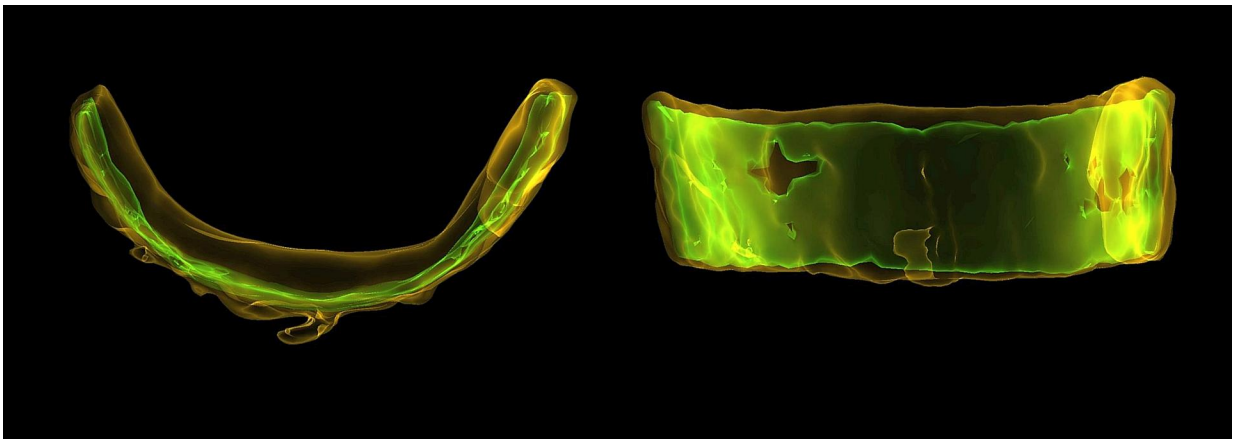


Figure 13: 3D CT of metallic neck implant in semi-transparency showing eccentric inner core with higher CT value (*in green colour*).

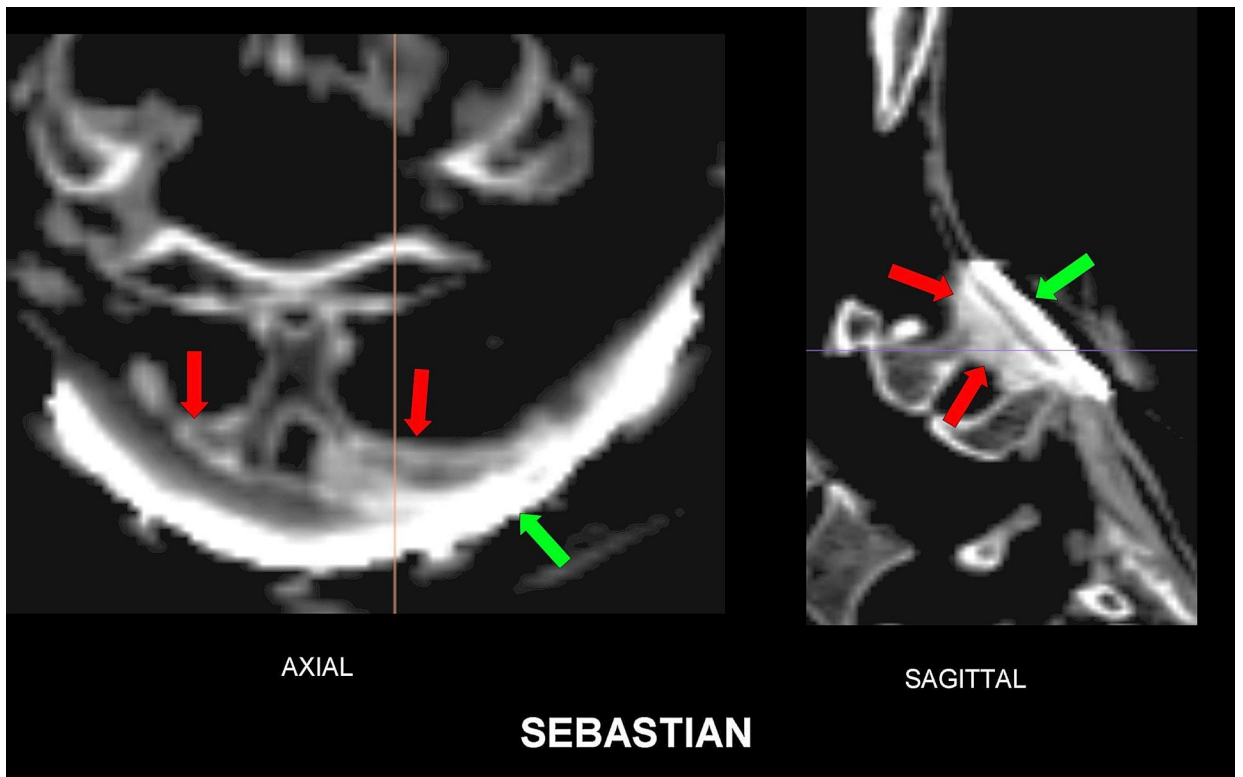


Figure 14: 2D axial (*left*) and sagittal (*right*) CT scans showing new bone formation (*red arrows*) from spinous processes of C2 and C3 incorporating into the collar like metallic implant (*green arrow*) in posterior neck indicating a functional implant.

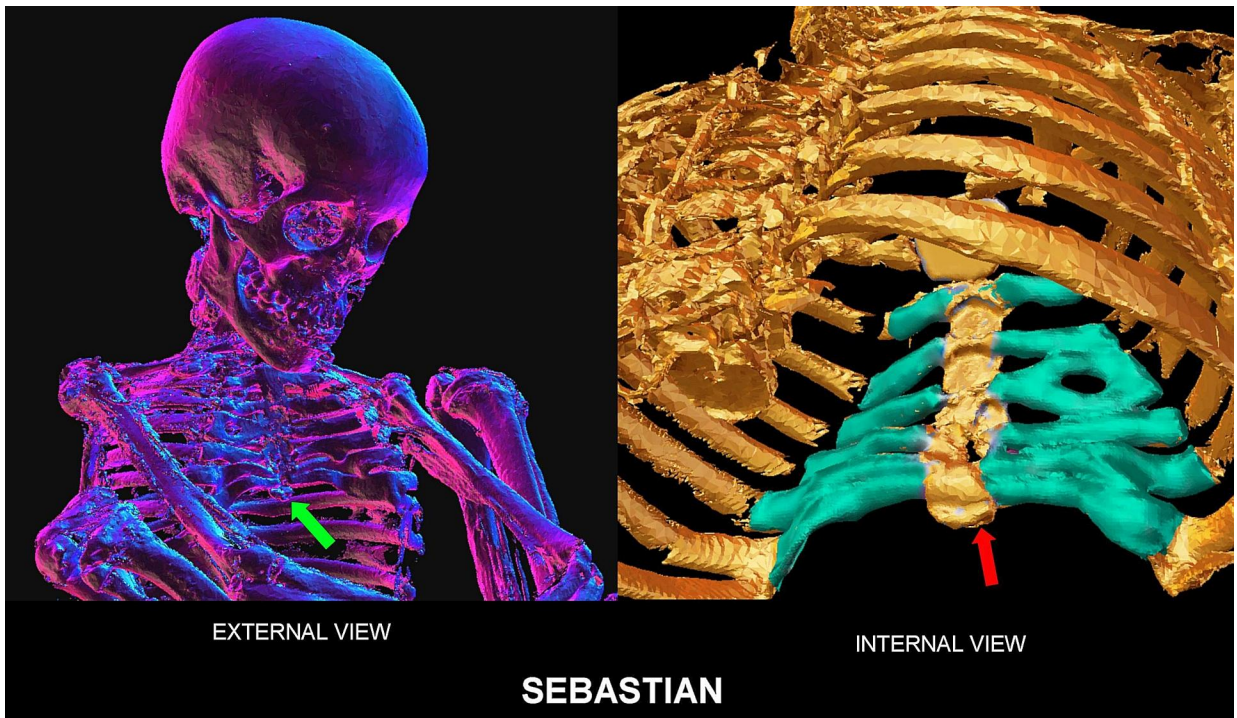


Figure 15: 3D CT of thoracic cage highlighting deformed, horizontally orientated robust costal cartilages with U-shaped deformity causing pectus excavatum. *Arrows* point to xiphisternum.



Figure 16: 2D sagittal CT scans showing heavily calcified intervertebral disks (*red arrows*) that showed higher density as compared with bone in thoracic (*left*) and lumbar (*right*) spine.

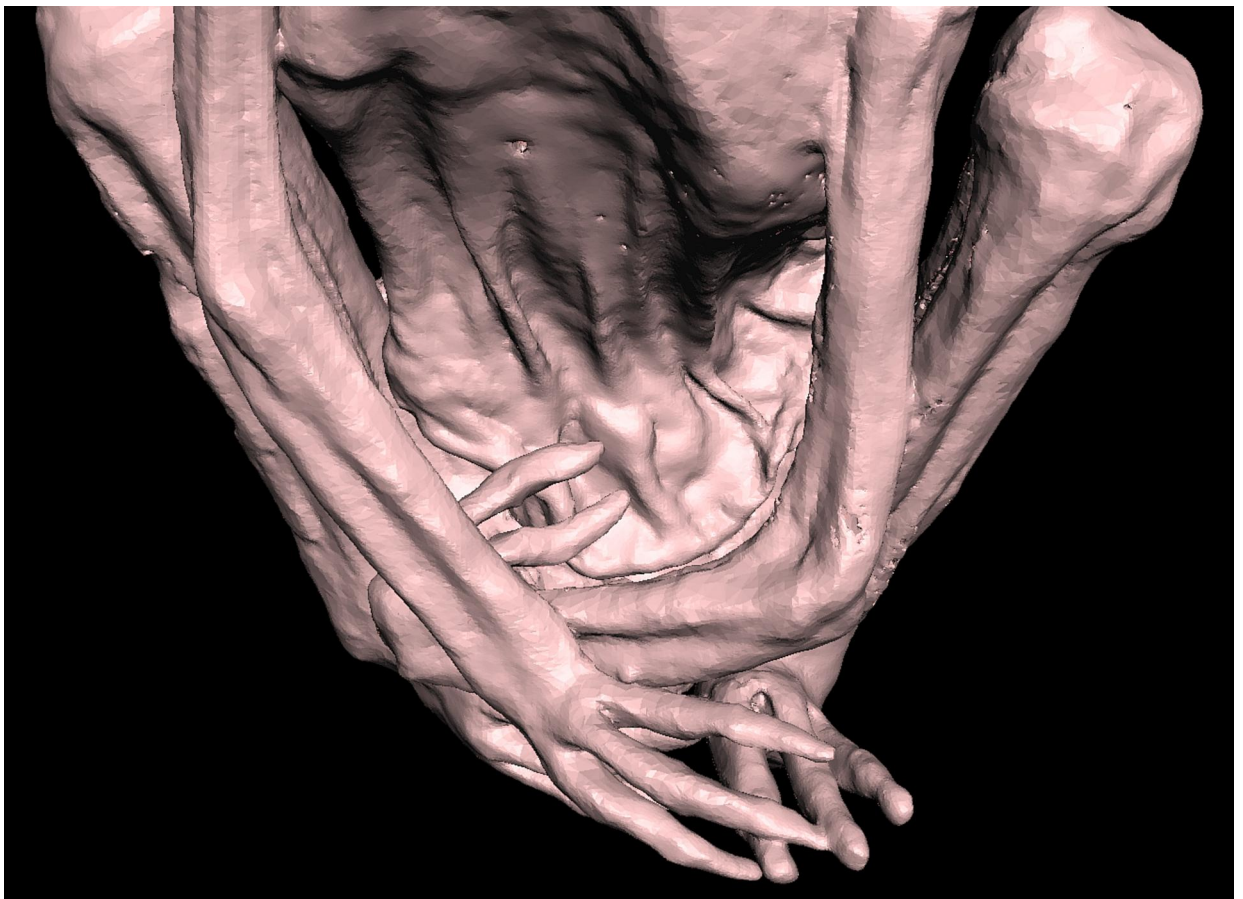


Figure 17: 3D CT showing prominent median abdominal fold and absence of navel.

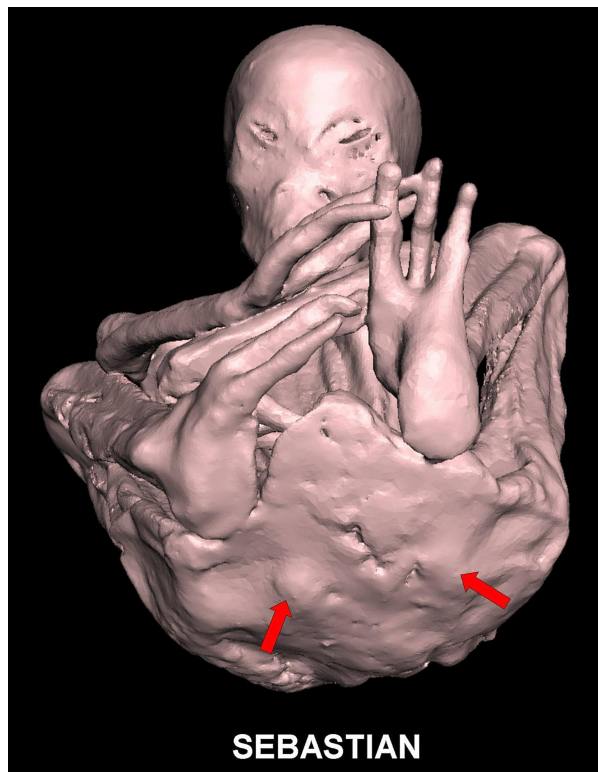


Figure 18: 3D CT showing flat triangular shaped perineum with lack of buttock prominences. Position of ischial tuberosities are marked. *(red arrows)*



Figure 19: 3D CT showing 'rocker bottom foot' deformity in left foot.



Figure 20: 2D coronal CT scan showing seeds within coprolites. (*red arrows*)

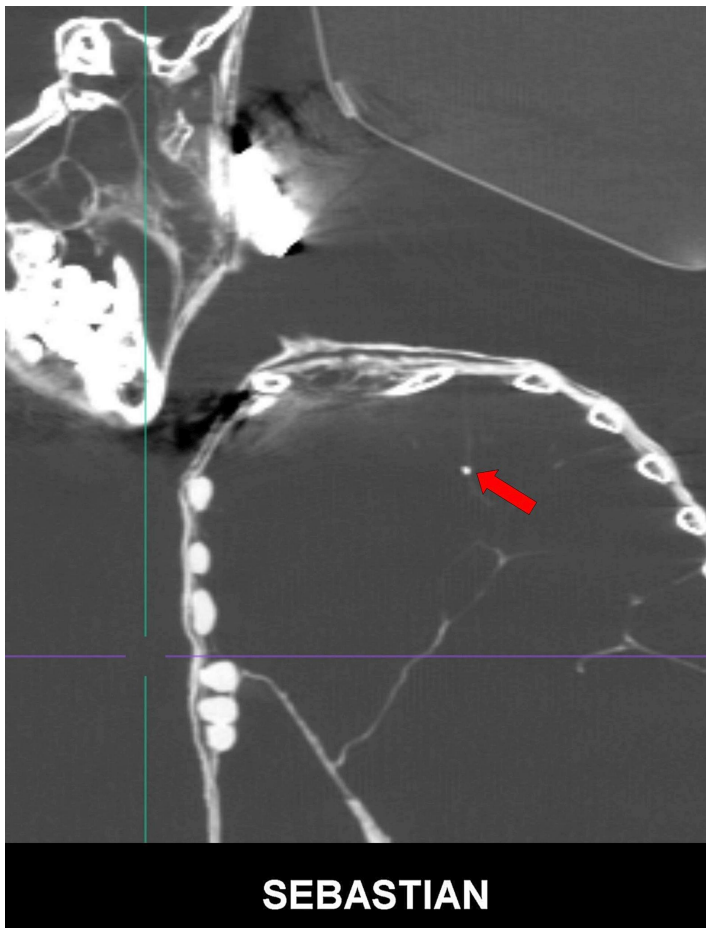


Figure 21: 2D sagittal CT scan showing calcified focus (*red arrow*) in upper lobe of left lung. Possibility of inactive pulmonary tuberculosis cannot be ruled out.



Figure 22: 2D coronal CT scan of sacrum showing well defined bony defect (*red arrow*) in left side of sacrum suggestive of Tarlov cyst.

SECTION III: EVIDENCES OF TRAUMATIC INJURIES IN ‘SEBASTIAN’

- A well defined triangular shape area of soft tissue and bone loss with clean sharp margin was noted in left posterior iliac region. This was related to recent biopsy site for tissue sampling. *(Figure 23)*
- A well defined triangular shaped puncture hole was found in lateral aspect of left lower neck. *(Figure 24)* The puncture hole led into a wide tract stretching across left side of neck ending anterior to C4 vertebra. *(Figure 25, 26)* A tiny metallic foreign body was found at the deep end of the tract anteriorly. *(Figure 26)* Associated hematoma was noted surrounding the tract, around mid cervical spine bilaterally and extending posterior to left paraspinal region and bilateral subcapital region above the metallic neck implant. *(Figure 25)* Bony destruction with anterior displacement and rotary subluxation of C4 was noted. *(Figure 27)*
- Associated epidural hematoma was noted in anterior spinal canal between C5 to T3 levels. *(Figure 28)*
- Two tiny metallic foreign bodies or focal calcifications were noted in spinal canal on right side at mid and lower thoracic levels. *(Figure 29)*
- Heart was partially collapsed. *(Figure 30, 39)*
- Deep wound with tissue loss was noted anteriorly medial to right shoulder. *(Figure 31)* The lateral part of upper epiphysis of right humerus was defective. *(Figure 31)*
- Wound with tissue loss were noted in right supraclavicular area medial and lateral to the metallic implant in that area. *(Figure 32)*
- Puncture wound was noted in left supraclavicular area lateral to the metallic implant in that area. *(Figure 32)*
- A puncture wound was noted in right scapula below scapular spine. *(Figure 33)*
- Smaller wounds with tissue loss were noted in upper anterior aspect of right thigh, mid anterior left thigh, anterior upper and posterior lower right leg. *(Figure 33, 34)*
- Lateral ends of bilateral clavicles were dislocated and in contact with humeral heads. *(Figure 35)*
- Posterior and inferior dislocation of bilateral femoral heads were noted. *(Figure 36)* Femoral heads were normal looking.
- Hyper-flexion in left wrist was noted. *(Figure 37)*
- Lungs were hyperinflated with depressed hemi-diaphragms. There was evidence of bilateral haemothoraces and subphrenic hematoma crossing midline from right side. *(Figure 38, 39)*
- Impression markings on bilateral loin. *(Figure 40)*
- Dislocations in left 6th, 7th, 10th, 11th costo-chondral junctions. *(Figure 41)*



Figure 23: 2D axial CT scan (*left*) and 3D CT (*right*) showing large defect (*red arrows*) in bone and soft tissue over left posterior iliac area due to biopsy.

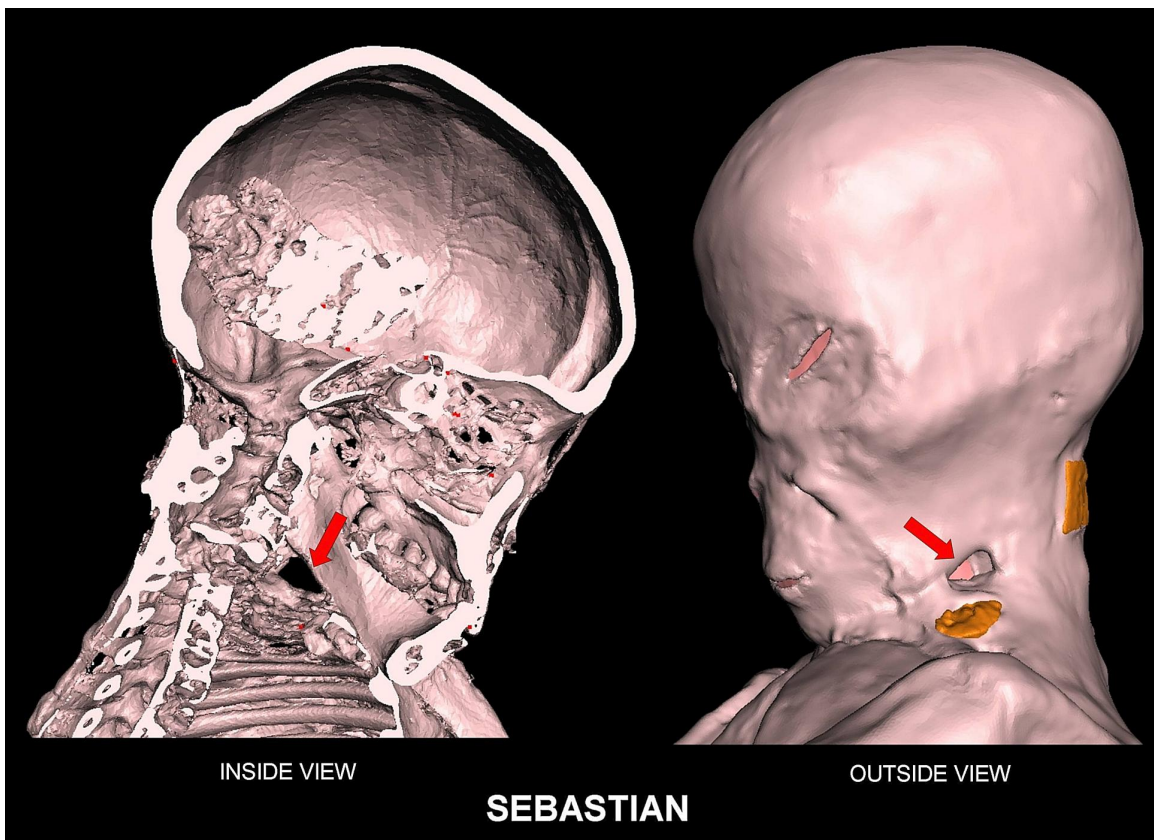


Figure 24: 3D CT showing inner (*left*) and outside (*right*) views of triangular shaped large puncture hole (*red arrow*) in left lower neck.

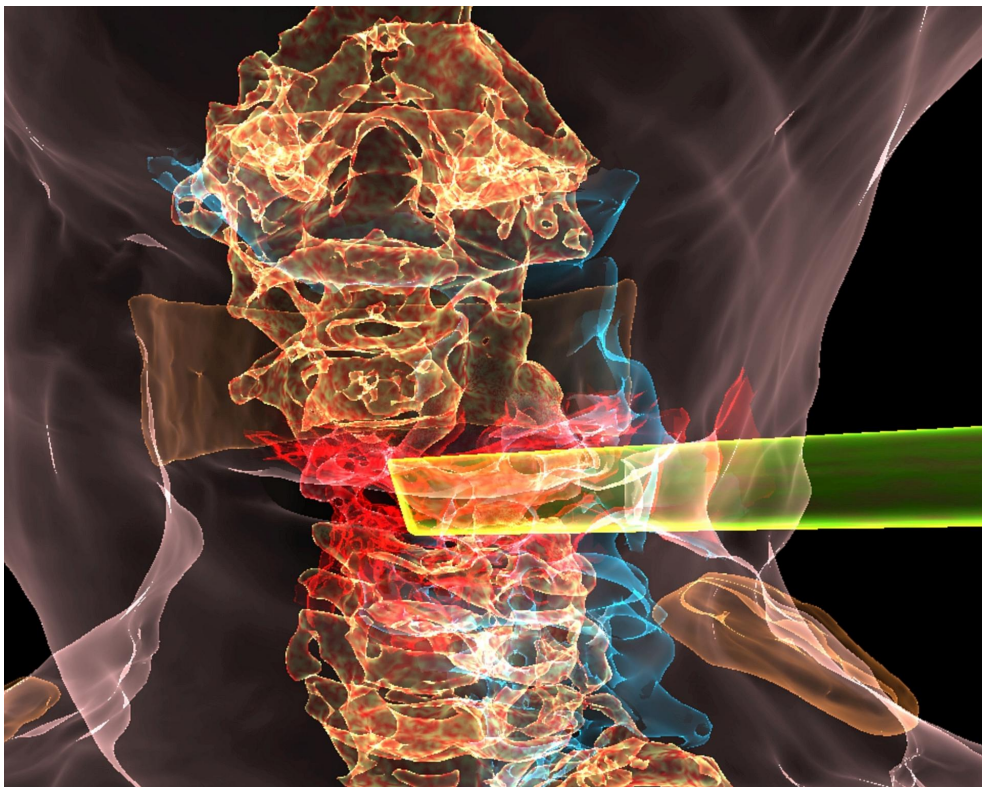


Figure 25: 3D CT frontal view showing proposed trajectory of penetrating object (*in green*), tissue tract (*in red*), associated hematoma (*in blue*) and cervical spine (*in orange*).



Figure 26: 2D coronal (*left*) and sagittal (*right*) CT scans showing wide tissue tract in neck (*green arrows*) with presence of small metallic foreign body (*red arrow*) at its inner end.

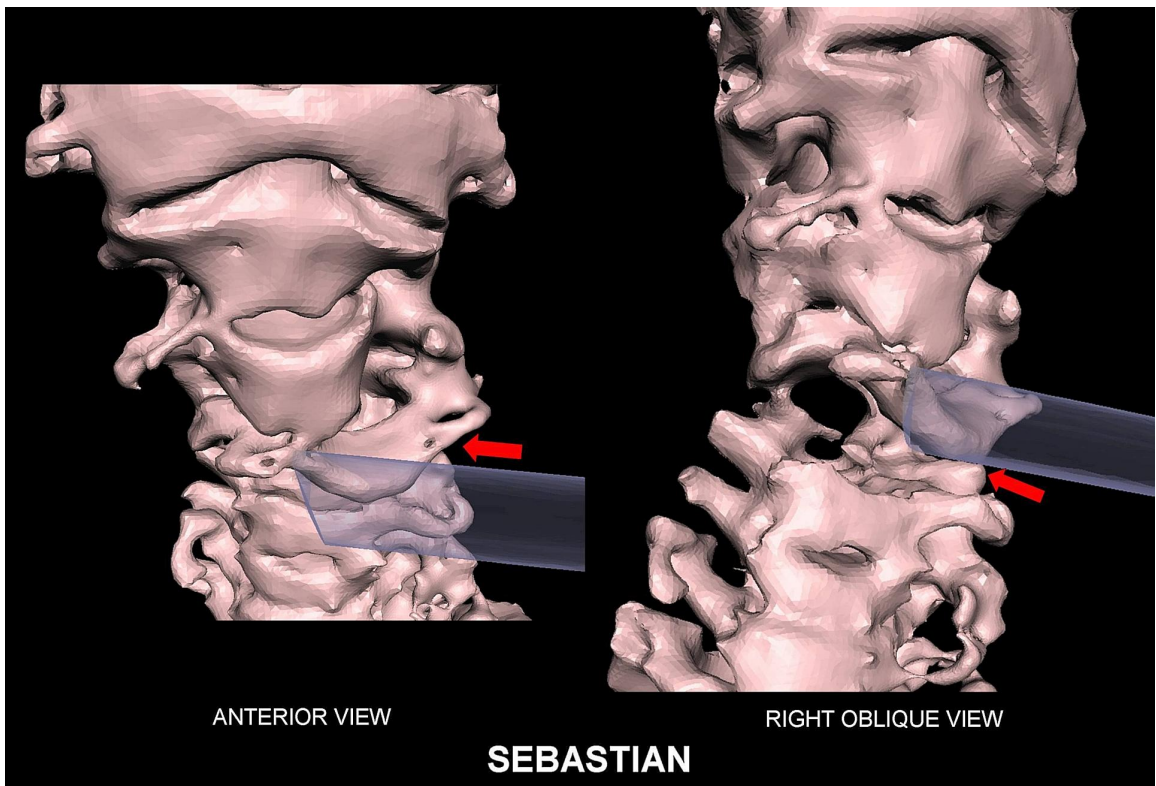


Figure 27: 3D CT showing frontal (*left*) and right oblique (*right*) views of cervical spine. Anterior displacement with rotary subluxation of C4 vertebra (*red arrow*) was evidence. Proposed trajectory of injuring object was shown in semi-transparency.

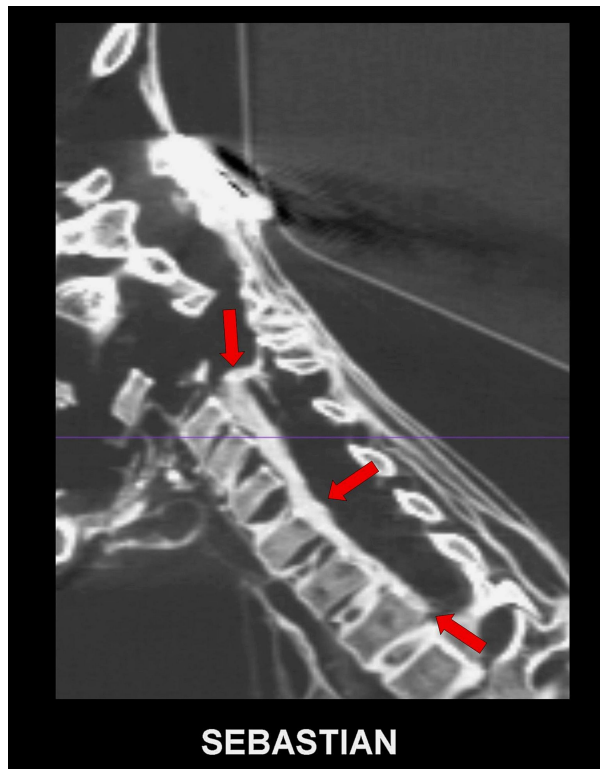


Figure 28: 2D sagittal CT scan showing epidural hematoma in anterior part of spinal canal related to C4 spinal injury extending from C5 to T3 levels.

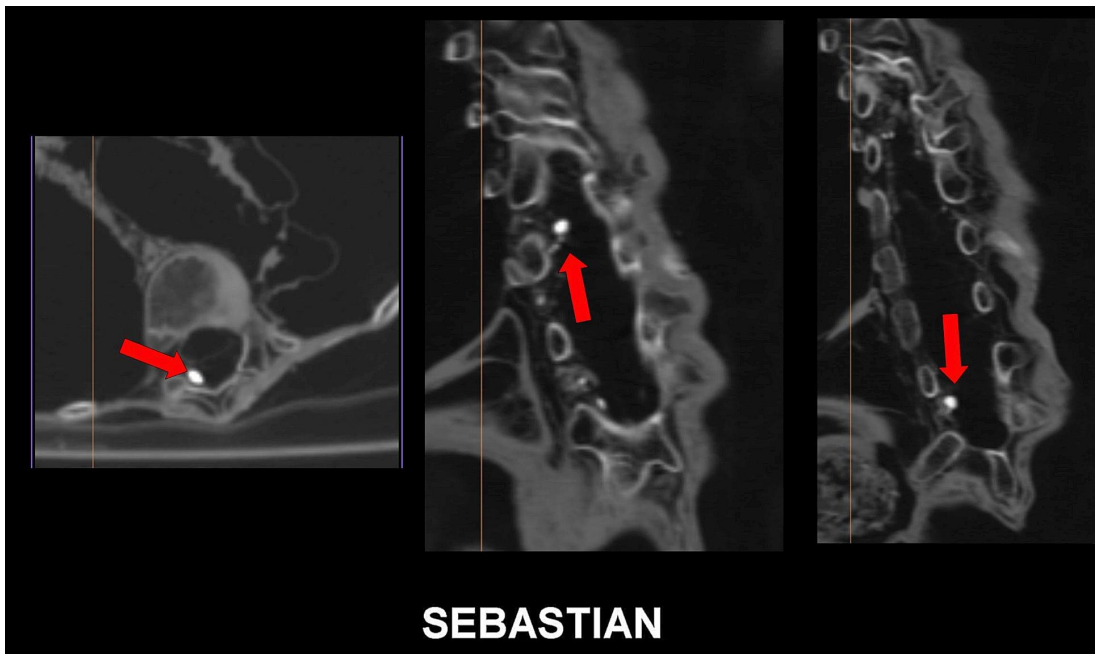


Figure 29: 2D CT scans in axial (*left*) and sagittal (*middle and right*) projections showing 2 metallic foreign bodies or calcifications (*red arrows*) in mid and lower thoracic spine.



Figure 30: 2D axial CT scan showing partially collapsed heart (*red arrows*).

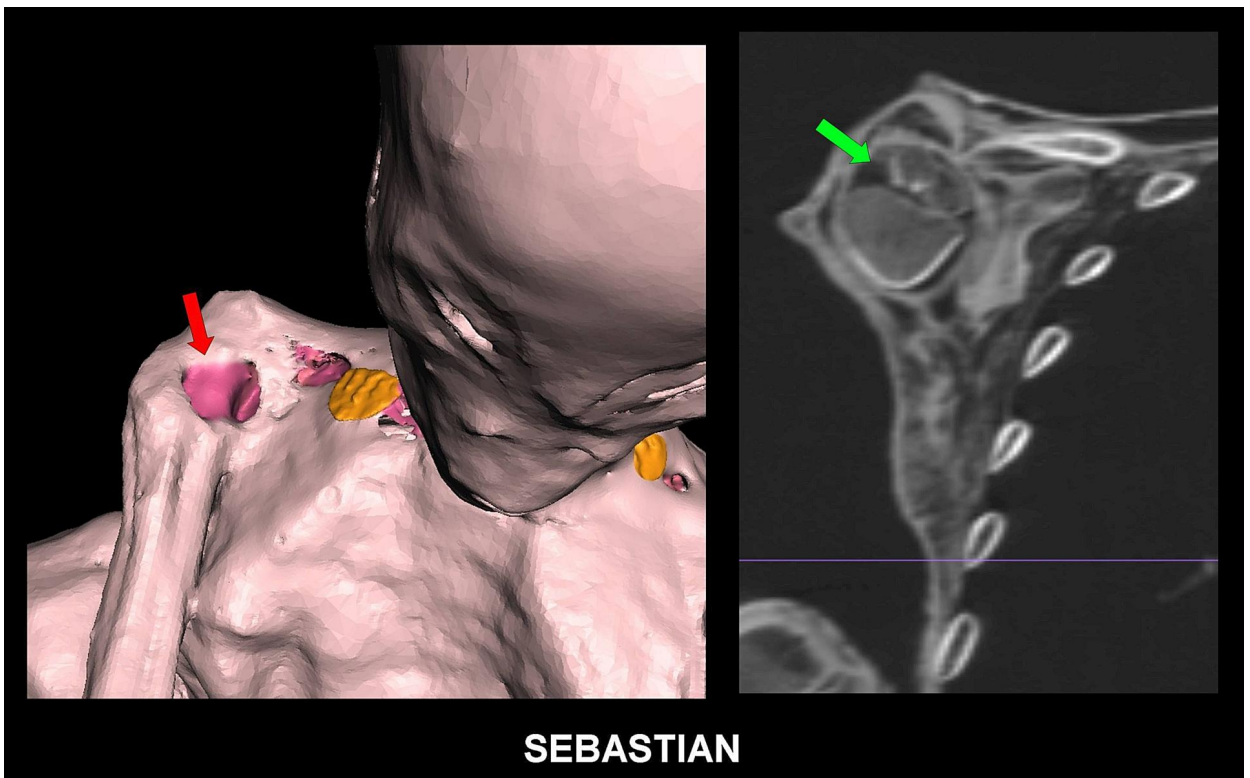


Figure 31: 3D CT (*left*) showing tissue loss (*red arrow*) over anterior medial aspect of right shoulder. Underlying destruction in lateral part of right upper humeral epiphysis (*green arrow*) can be found on 2D coronal CT scan (*right*).

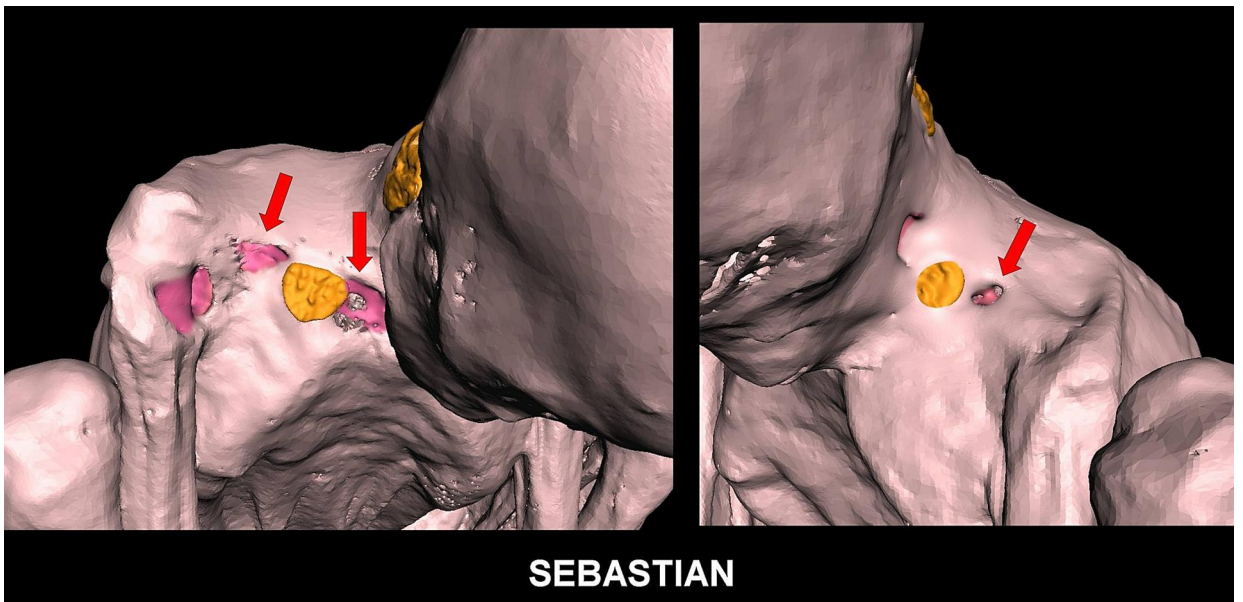


Figure 32: 3D CT showing tissue loss (*red arrow*) over right supraclavicular area (*left*). Puncture wound (*red arrow*) was noted lateral to metallic implant in left supraclavicular area (*right*).

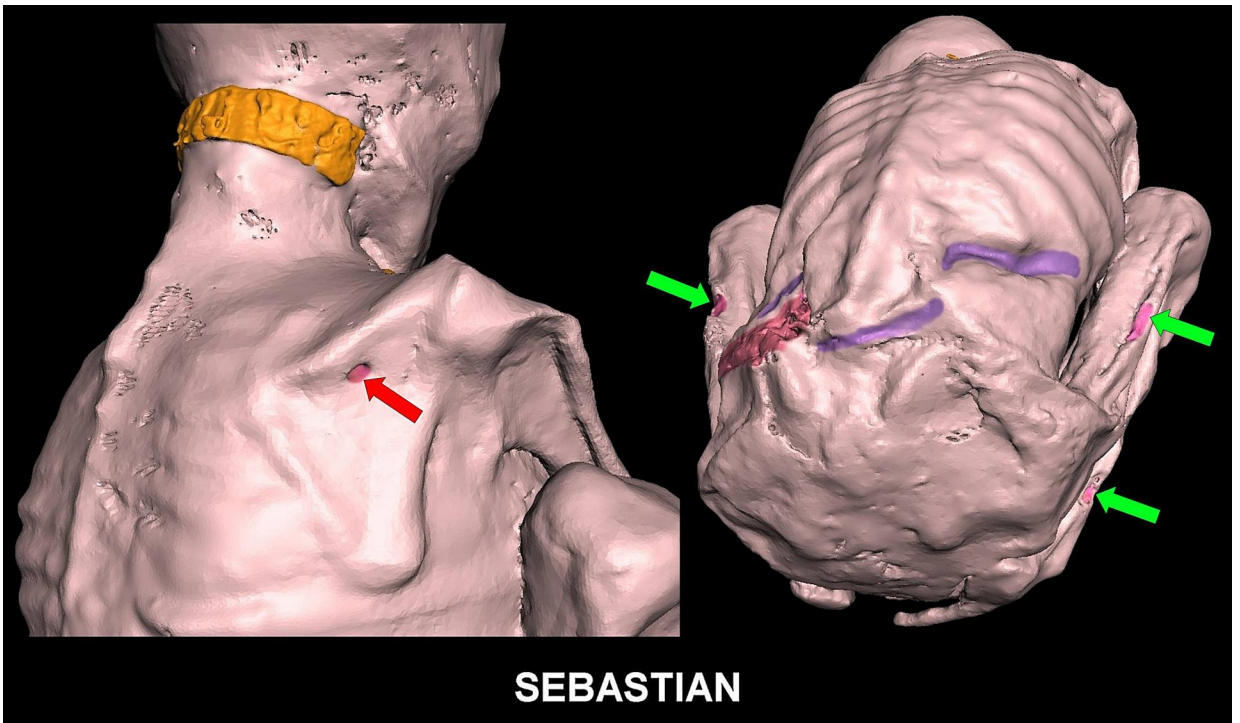


Figure 33: 3D CT showing puncture wound (*red arrow*) below right scapular spine (*left*). Areas of tissue loss (*green arrows*) were found in bilateral thighs and right leg (*right*).



Figure 34: 3D CT showing wound (*red arrow*) in right shin.



Figure 35: 2D coronal CT scan showing right shoulder (*left*) and left shoulder (*right*) both showing lateral ends of clavicles (*red arrows*) located below acromial processes (*green arrows*) and in contact with humeral head (*H*) suggestive of dislocation.



Figure 36: Recreated 3D models of pelvis and both hips based on 3D CT showing dislocation of both femoral heads (*red arrows*) from acetabuli.



Figure 37: Bilateral hands and wrists showing hyper-flexion in left wrist. This could indicate hyper-mobility of the wrist joint or result of trauma.



Figure 38: 2D CT scans in frontal projections showing presence of hyper-inflated lungs with depressed hemi-diaphragms and presence of bilateral hemo-thoraces (*red arrows*). Subphrenic hematoma (*green arrow*) crossing midline from right side was also noted.

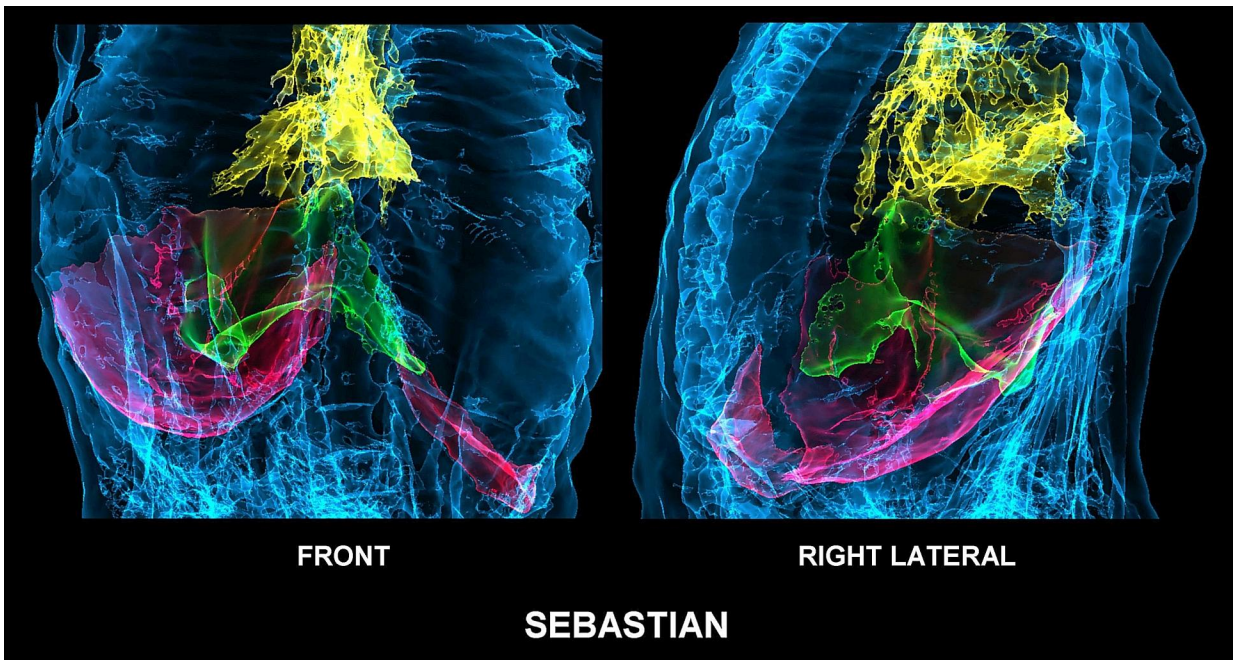


Figure 39: 3D CT showing depressed hemi-diaphragms with bilateral hemo-thoraces (*in red*) and subphrenic hematoma (*in green*). Heart (*in yellow*) appeared partially collapsed.

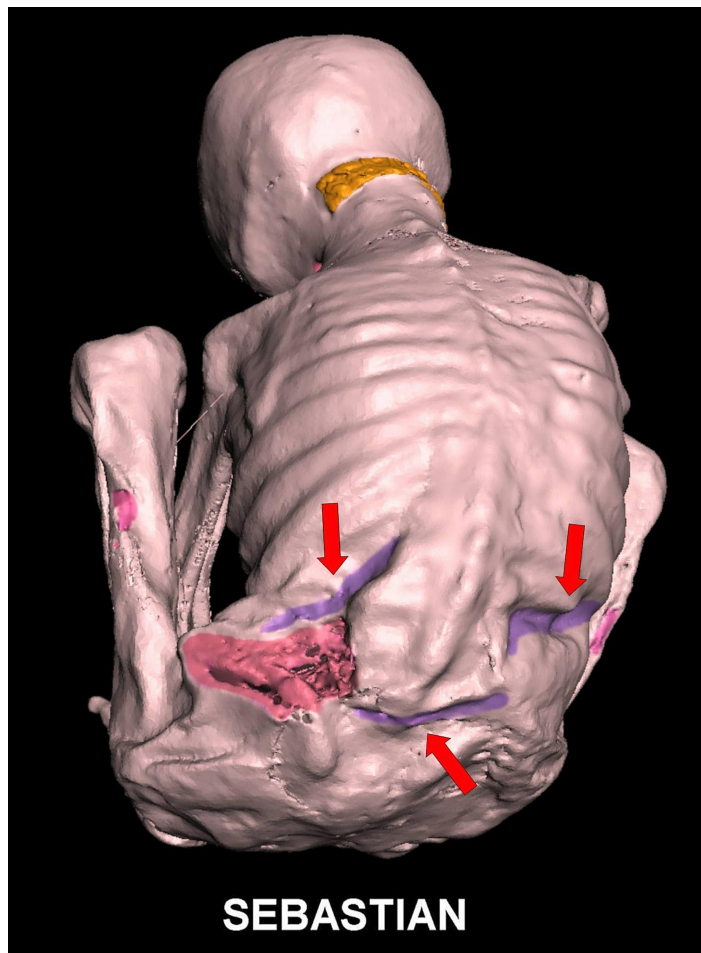


Figure 40: 3D CT showing presence of deep band shaped (*in purple*) impressions (*red arrows*) on skin surface of bilateral loins and above sacral area.

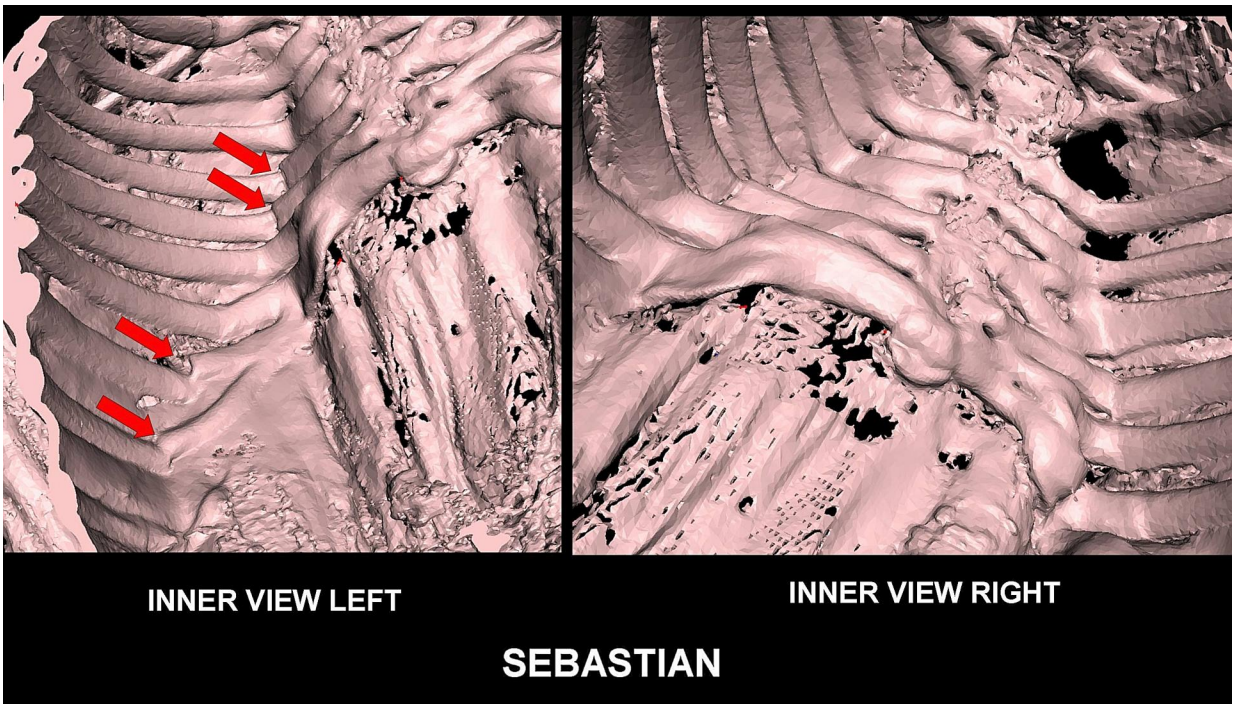


Figure 41: 3D CT showing inner aspect of thoracic cage. Subluxations were seen in left 6th, 7th, 10th and 11th costochondral junctions (*red arrows*).

SECTION IV: CONCLUSION

- CT evidences suggested that ‘Sebastian’ is a genuine dehydrated corpse with comprehensive integrated anatomy. As anatomical specimen, it surpasses the Egyptian mummy in details of internal anatomy and tissue preservation.
- CT evidences show beyond doubt that ‘Sebastian’ had been a previously living biological entity. The find of ‘Sebastian’ and related tridactyl corpse is of great significance in anatomy, archaeology, anthropology, history, culture, medicine, metallurgy, method of preservation of tissue preservation and in natural sciences.
- ‘Sebastian’ can be considered to be a bipedal hominid. Together with other similar tridactyl hominids e.g. ‘Montserrat’ and ‘Maria’ found in Peru, it shared a group of similar anomalous features not reported in known syndromes in human. The term ‘TRIDACTYL SYNDROME’ is proposed to describe the set of abnormalities. ‘Sebastian’ can be a representative example of the syndrome with anomalies including lack or fused cranial sutures, abnormal shaped skull, enlarged foramen magnum, large orbits with widely separated slanting eyelids, small or absent nose, absent or abnormal orientation of nostrils, absent pinnae, small facial bones, small prominent jaw with pointed cheek, pectus excavatum with robust deformed costal cartilages, calcified intervertebral disks, prominent median fold in anterior abdominal wall, triangular shaped perineum with flat buttocks with tridactyls being the hallmark feature.
- ‘Sebastian’ has 2 disk shaped metallic implants overlying bilateral clavicles and a collar shaped metallic implant behind the neck. A clinically very significant finding is the presence of florid new bone formation from cervical spine that fused with the implant.
- Seeds were found in the coprolites suggesting a plant based diet.
- Disease processes were found including Tarlov cyst and presence of lung calcification (that may signify non-active pulmonary tuberculosis).

SECTION IV: CONCLUSION *(continue)*

□ ‘Sebastian’ had suffered from extensive external and internal injuries. Major injury is found in the neck with presence of a large triangular shaped puncture hole suggesting entrance wound of a large sized penetrating object that cause disruption of not only soft tissue but also causing bone damage and dislodgement of the C4 vertebra. No exit hole was found. There is evidence of extensive bleeding around the injured site and extending to the whole neck. This penetrating injury could have been life threatening. There were evidences of blunt trauma (e.g. impression marks on back, subluxation in costochondral junction) that could have caused internal hemorrhage (bilateral haemothoraces and subphrenic hematoma). ‘Sebastian’ may have succumbed to blood loss following major trauma as evident by the partially collapsed heart.

CAUSE OF DEATH: MAJOR TRAUMATIC INJURIES WITH BLOOD LOSS

SECTION V: CAUSE OF DEATH

‘Sebastian’ died a traumatic death from severe blood loss due to large penetrating injury in left side of neck as well as bleeding from internal injuries

ABOUT DR. FUNG

Dr. K H Fung is a retired radiologist with over 40 years of experience in diagnostic radiology. His special interests include 3D medical visualization, interventional radiology and neuro-intervention.

Dr. Fung is also an artist in the domain of intersection of art and science utilising his expertise in 3D medical visualization. Dr. Fung was the first place co-winner in the '2007 International Science & Engineering Visualization Challenge' organized by Science magazine and National Science Foundation (USA).

His artworks had been exhibited in museums in various countries including USA, Europe, China, Australia and Hong Kong.

He had current exhibits in 2025 in the Hong Kong Museum of Medical Sciences (featuring stereoscopic 3D and 4D medical imaging and art) and in Nina Park (featuring the Nina wood fossils collection) in Hong Kong.

Through his collaboration with Science Photo Library, his interdisciplinary artworks bridging art and science had been made available to various international renowned digital media, magazines, books, and journals.

/end